

Miniature Folded Dipole in Rotational Symmetry for Metal Tag Design

Shao-Ming Chiang, Tong-Lin Lee, Eng-Hock Lim^{*}, Pei-Song Chee, Yong-Hong Lee, Fwee-Leong Bong, Yeong-Nan Phua, and Boon-Kuan Chung

Abstract—In this paper, a miniature folded dipole is proposed for designing a metal-mountable UHF RFID tag. The proposed tag antenna is low in profile and has a compact size of $40\text{ mm} \times 40\text{ mm} \times 3.1\text{ mm}$ ($0.122\lambda \times 0.122\lambda \times 0.009\lambda$). Folding the dipole arms into a two-fold rotational symmetrical style can miniaturize the tag footprint for achieving high compactness. It has been found that the capacitive coupling mechanism between the rotational symmetrical radiating arms is effective in enhancing the vertical radiation, which subsequently improves the achievable read distance in the boresight direction. Also, an incorporated circular loop can provide additional inductance for achieving good impedance matching with the RFID chip. For the proposed tag antenna, a full ground plane is inserted underneath the radiator for isolating it from the backing metal, making the tag tolerant to the metallic platform. The proposed tag antenna is able to achieve a maximum read distance of 7 m at 4 W EIRP when it is tested on metal.

1. INTRODUCTION

RFID technology has expanded multifold over the years, and it has been adopted by many practical applications such as electronic toll collection, animal tracking, and logistics management [1]. Unlike barcode and QR code systems, an RFID reader can identify multiple tags within its wireless range simultaneously. It makes the RFID system much more efficient and cost-effective. Moreover, a single RFID tag can be reused for many times by simply reprogramming the microchip on the tag, which greatly reduces implementation costs [2]. Passive RFID systems working in the ultrahigh-frequency (UHF) band have gained much attention recently because they are able to provide long read distance and large memory capacity at a low cost. However, it is very challenging for a UHF tag antenna to maintain good performances when it is placed near a metal object. Significant degradation in antenna's radiation performances can occur due to the effects of its own opposite image currents [3]. Most of the commercial metal tags, which are usually made of dipole, have a large footprint, and they can barely provide far read distance [4]. In [5], the achievable read distance of a multi-arm tag antenna could deteriorate significantly when it was tested on a metal plate. Similar effects were also reported in [6]. Degradation in the radiation performances in the presence of a conductive platform is a severe problem. Some researchers have proposed to incorporate metamaterials such as electromagnetic bandgap (EBG) and artificial magnetic conductor (AMC) into the antenna design for reducing the effects of the opposite image currents [7, 8]. According to [7, 8], EBG and AMC could selectively suppress the surface electromagnetic waves by varying the phase of the reflected waves from -180° to 180° , depending on the frequency. Such suppression allows the conventional antennas to work without much deterioration in performances even though they are placed in proximity to the conductive materials.

Received 6 December 2020, Accepted 5 February 2021, Scheduled 17 February 2021

^{*} Corresponding author: Eng Hock Lim (limeh@utar.edu.my).

The authors are with the Department of Electrical and Electronic Engineering, Lee Kong Chian Faculty of Engineering and Science (LKCFES), Universiti Tunku Abdul Rahman, Kuala Lumpur, Malaysia.

Nevertheless, complicated design and high fabrication costs have remained as the main problems for utilizing metamaterials for tag design.

Antenna size is another important criterion for designing an RFID tag as a large tag cannot be really used for many practical applications. Several common miniaturization techniques can be found in literature, such as meandering the radiating arms [9] and introducing slots/notches to the radiator [10, 11]. Although meandering the radiating arms can lower the footprint, it has adverse effect on the radiation efficiency and antenna bandwidth, which can be caused by current crowding effect [12]. As reported in [13], a meandered folded dipole could be realized with a size of much smaller than $\lambda/2$. However, its achievable read distance was also deteriorated to 3.01 m when the antenna was tagged on a metal with a 1 mm spacer. It was demonstrated in [14] that introducing slots on a radiator was useful for increasing the current paths and, thus, enhancing the reactance for achieving miniaturization. However, the engraved slots or notches were also radiating, and the fields could interfere with the main radiation. Using high-permittivity substrates [15] to lower the operating frequency appears to be one of the possible alternatives for miniaturization. However, high-permittivity substrates are usually not cheap, and this way may not be cost-effective for practical tagging applications.

In this paper, a folded dipole antenna has been proposed for designing a metal-mountable UHF RFID tag, with the characteristics of low profile, high gain, long read distance, and platform-tolerance. Folding a dipole into a two-fold rotational symmetry, rather than meandering it, is found to be able to scale down the tag size without compromising radiation performances [16]. It will be shown later that the read distance of the proposed tag antenna is much farther than most of its contemporary counterparts [5, 17]. Moreover, the radiating arms are able to provide multi-degrees of tuning freedom, which makes the tuning process much simpler. As such, the antenna structure does not need additional inductive stubs/vias, which can increase the fabrication complexity, to achieve conjugate match with the chip. Besides, the proposed structure has a ground plane underneath which acts as an electromagnetic shield to make it a platform-tolerant antenna. This paper consists of 6 parts. In Part 2, the configuration of the proposed tag antenna and field distributions are studied. Here, the design steps will be discussed. The equivalent circuit will be proposed for analyzing the characteristics of antenna impedance. An analysis on the crucial parameters will be included in Part 3. In Part 4, the prototype fabrication and measurement setup will be briefly described. Measurement results including tag sensitivity, realized gain, and reading patterns will be discussed in Part 5. A conclusion is drawn at the end.

2. ANTENNA CONFIGURATION

The proposed miniature dipole is designed and simulated using the CST Microwave Studio. With reference to Fig. 1(a), the radiating arms of the dipole on the top layer are rotationally folded in the counterclockwise direction, and they are trimmed into square shape for ease of fabrication. The tag antenna is electrically small, and it has a size of 40 mm \times 40 mm. Folding the arms, rather than meandering, is able to keep the undesired current crowding effect at minimum [12]. Arranging the two expanded arms in rotational symmetry for occupying the opposite corners is able to enhance the radiation performances effectively [16]. The coupling mechanism between the two expanded arms is also able to introduce additional shunt capacitance to the antenna impedance for tuning down the resonant frequency to the desired range. Here, the radiating arms are intentionally divided into multiple nonuniform segments so that they can be varied for tuning the resonant frequency. A circular matching loop located at the center is used to join the dipole arms and to provide additional inductive reactance to the antenna impedance for improving the matching [18]. A small gap (c_1) located on the matching loop is reserved for accommodating the RFID chip [19]. Referring to Fig. 1(b), the proposed antenna has its own backing ground plane on the reverse side to function as an electromagnetic shield for minimizing the impact of the conductive platform. Moreover, the added ground plane is able to provide capacitive loading effect which is useful for tuning down the resonant frequency to the desirable UHF band [20]. It is worth mentioning that the proposed antenna does not have any shorting vias/stubs, which require additional printed-circuit-board (PCB) drilling or milling processes.

The design parameters of the proposed tag antenna are optimized using a software-embedded optimizer, and the values are found to be: $a_1 = 12.00$ mm, $a_2 = 18.90$ mm, $a_3 = 12.00$ mm, $b_1 = 5.85$ mm, $b_2 = 4.00$ mm, $b_3 = 3.80$ mm, $b_4 = 13.10$ mm, $b_5 = 37.00$ mm, $c_1 = 0.50$ mm, $d_1 = 4.10$ mm,

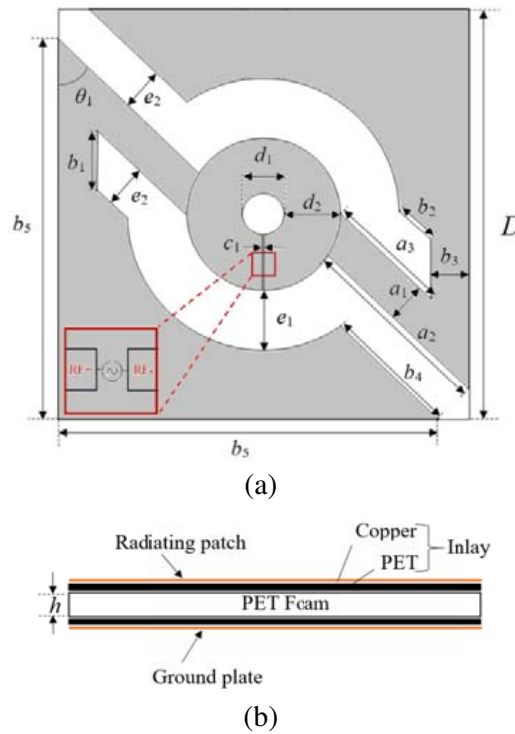


Figure 1. (a) Configuration of the proposed tag antenna. (b) Side view of the tag antenna structure.

$d_2 = 5.40$ mm, $e_1 = 5.85$ mm, $e_2 = 4.20$ mm, and $\theta_1 = 46.56^\circ$. Subsequently, the optimized structure is fabricated by etching a copper foil ($9\ \mu\text{m}$) which was initially deposited on a single-layered flexible thin PET film (polyethylene terephthalate, $50\ \mu\text{m}$). Then, the completed inlay is folded symmetrically around a flexible foam ($\epsilon_r = 1.06$, $\tan \delta = 0.0001$) [21] with a size of $40\ \text{mm} \times 40\ \text{mm} \times 3\ \text{mm}$, as illustrated in Fig. 1(b). Using flexible materials for fabrication, rather than rigid structures, makes the antenna easily conformal when the tag is mounted on an uneven surface.

The design process is started by specifying the microchip and materials. An Impinj Monza R6 chip, which has an impedance of $12 - j119.5\ \Omega$ [19], is selected for the tag. The impedance of the antenna port is set to be the chip impedance in simulation. For achieving flexibility, the tag is designed using the PET film and foam material. The tag size is set to be $40\ \text{mm} \times 40\ \text{mm} \times 3\ \text{mm}$. In all the subsequent design steps, the tag antenna is placed at the center of a $20\ \text{cm} \times 20\ \text{cm}$ metal plate, which has a thickness of 1 cm. With the use a foam substrate ($40\ \text{mm} \times 40\ \text{mm} \times 3\ \text{mm}$), a simple straight dipole ($50\ \text{mm} \times 3\ \text{mm}$), which is named as *Configuration A*, and it has a ground plane on the reverse side of the foam, is designed on a single-layered PET film. The dipole is aligned along the diagonal of the square footprint, as can be seen in the right inset of Fig. 2(a), for achieving a maximum length. In this case, the tag resonant frequency is found to be 3340 MHz, which is too high for the UHF RFID design, with an antenna impedance of $8.74 + j119.5$. The corresponding power transmission coefficient (τ) is found to be 0.975, as shown in Fig. 2(b). To lower the frequency, as can be seen in the left inset of Fig. 2(a), the radiating arms of the dipole are meandered for increasing the dipole length from 50 mm to 136.4 mm. The new antenna is called *Configuration B*. With this increase, the resonant frequency has gone down to 1644 MHz. However, the antenna resistance has decreased significantly to $0.93\ \Omega$, as observed in Fig. 2(a), causing τ to jeopardize to 0.265 (Fig. 2(b)) due to poor impedance matching. It is observed from simulation that currents on the closely placed meandered arms interact with each other, causing crowding effect. To improve the impedance matching, T-match technique is employed by incorporating a circular matching loop. Here, the two radiating arms are connected to the two opposite sides of the loop in a rotational symmetry style, and this intermediate structure is named as *Configuration C*. In this case, as can be seen in the right inset of Fig. 3(a), the tag resonant frequency can be easily brought down to 980.6 MHz, and the antenna resistance has been successfully increased to 8, with a reactance

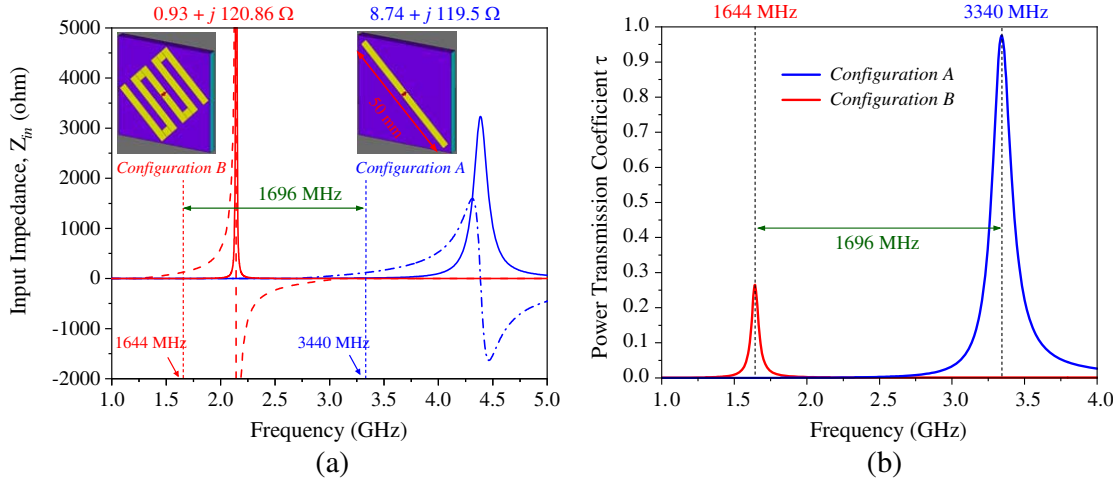


Figure 2. (a) Antenna impedances and (b) power transmission coefficients for *Configuration A* and *Configuration B*.

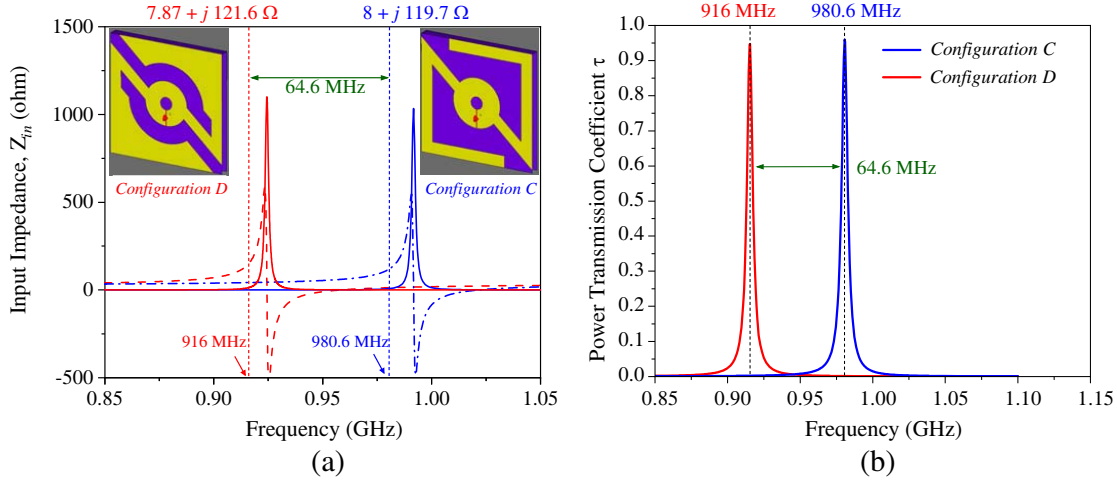


Figure 3. (a) Antenna impedances and (b) power transmission coefficients for *Configuration C* and *Configuration D*.

of 119.7. Due to the improvement in impedance matching, the power transmission coefficient has been significantly raised to 0.96, Fig. 3(b). To further fine-tune the frequency, the two radiating arms are broadened, and the tag resonant frequency (916 MHz) is now falling within the desired UHF passband, as shown in *Configuration D* (Fig. 3(b)), which is also our final tag configuration. With reference to Fig. 3(b), τ is 0.95 due to good impedance matching with the chip.

The surface current distributions of the proposed tag antenna are also simulated for studying the effect of the two-fold rotational symmetry on the radiation performances. As can be seen in Fig. 4, surface currents distributed on both the dipole arms are mostly in parallel, with higher current density found along the inner edges. It shows that the effect of current cancellation due to the oppositely induced currents is insignificant. It will be shown later that the proposed tag antenna is able to achieve a much longer read distance than those meandered structures. High current density is also found on the matching loop at the center, showing that the loop is useful for providing inductive loading to the antenna reactance. The electric and magnetic field distributions of the proposed tag antenna at the resonant frequency of 916 MHz are shown in Fig. 5. Referring to Fig. 5(a), strong electric fields are observed on the dipole arms, showing that the two-fold rotational symmetry design is able to improve the capacitive coupling. It can be used to tune down the resonant frequency for achieving miniaturization.

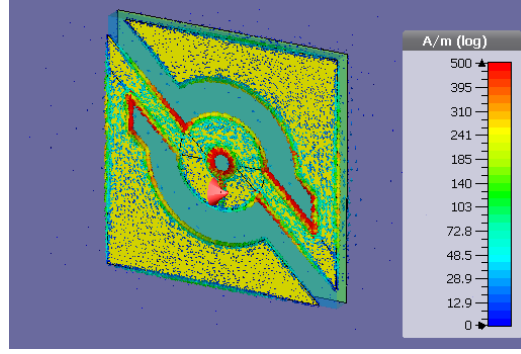


Figure 4. Surface current distribution on the tag antenna.

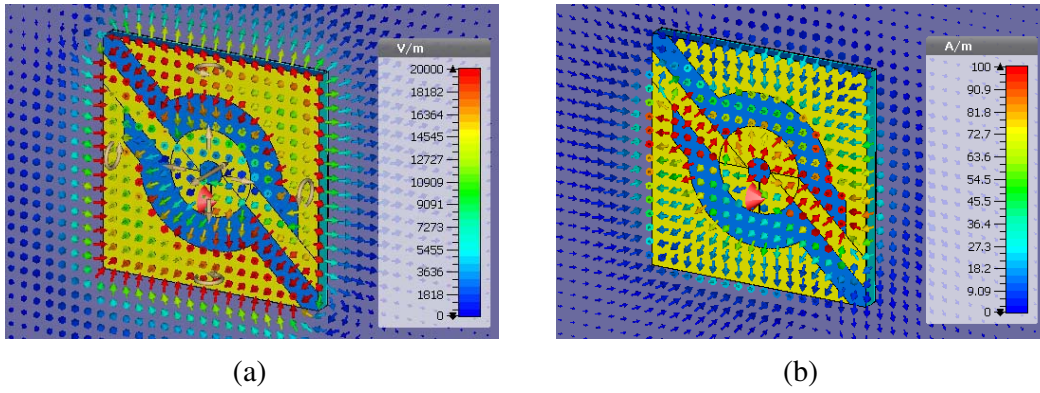


Figure 5. Simulated (a) electric field and (b) magnetic field distributions at resonance.

In addition, the electric field vectors are found to be pointing normally to the $+z$ direction, causing the back lobe to decrease considerably. This is desirable as it can make the proposed tag antenna less susceptible to the conductive platform, while enhancing the radiation in the boresight direction. Here, transverse magnetic field is found to be formed in between the top conductive layer and the ground plane underneath. This is nothing unusual for a patch-like planar dipole.

3. EQUIVALENT CIRCUIT MODEL AND PARAMETRIC ANALYSIS

The equivalent circuit model of the proposed design is shown in Fig. 6. The matching loop can be viewed as a resistance (R_m) and an inductance (L_m) in series, and they are in parallel with a capacitance (C_m). This is because strong electric fields have been observed in the broadened dipole arms, which can be regarded as capacitive loading. The radiator can be represented by a conventional RLC resonant circuit, and it is expressed as R_a , L_a , and C_a in series. With reference to the equivalent circuit model in Fig. 6, the input impedance of the tag antenna (Z_{in}) can therefore be expressed as follows:

$$Z_{in} = \frac{Z_a Z_m}{Z_a + Z_m} \tag{1}$$

where the impedances of the radiator (Z_a) and matching loop (Z_m) are given in Eqs. (2) and (3), respectively.

$$Z_a = R_a + j \left(\omega L_a - \frac{1}{\omega C_a} \right) \tag{2}$$

$$Z_m = \frac{R_m + j\omega (L_m - \omega^2 L_m^2 C_m - R_m^2 C_m)}{(1 - \omega^2 L_m C_m)^2 + (\omega R_m C_m)^2} \tag{3}$$

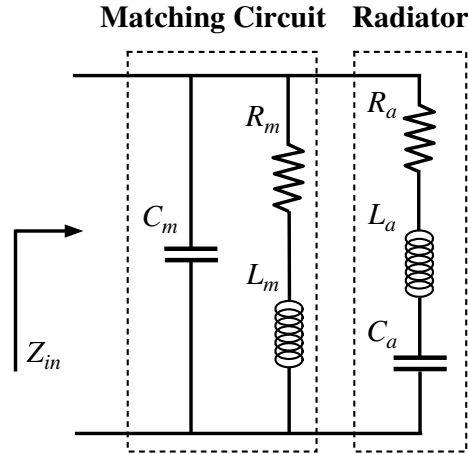


Figure 6. Equivalent circuit model of the proposed tag antenna ($R_m = 0.12 \Omega$, $L_m = 5.65 \text{ nH}$, $C_m = 0.24 \text{ pF}$, $R_a = 1.05 \Omega$, $L_a = 52.9 \text{ nH}$, and $C_a = 0.5 \text{ pF}$).

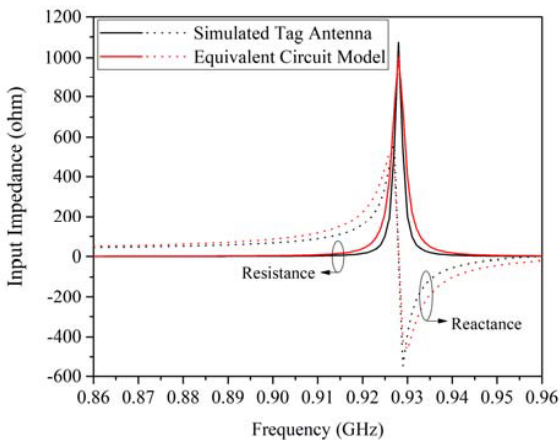


Figure 7. Simulated and modeled input impedance of the proposed tag antenna.

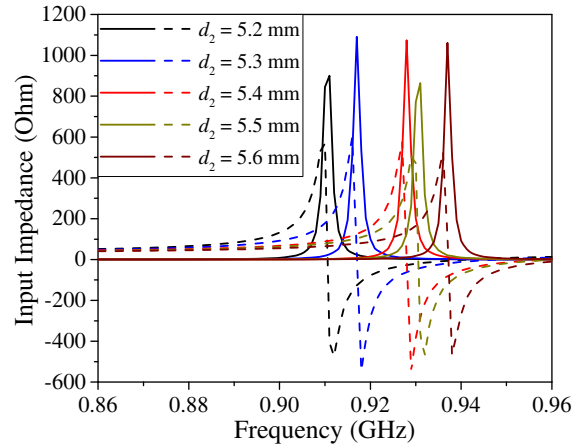


Figure 8. Effects of changing the matching loop's width (d_2) on the input impedance.

Figure 7 shows the input impedance of the proposed tag antenna. Referring to the same figure, the input impedance obtained using the derived equivalent circuit model matches well with its simulated counterpart, showing that the circuit model is suitable for describing the electrical properties of the tag antenna. At the resonant frequency of 916 MHz, the input impedance of the proposed tag antenna is $7.87 + j121.6 \Omega$, which is almost in conjugate match with the chip impedance of $12 - j119.5 \Omega$ [19]. The real part of the antenna impedance is found to be slightly lower than the chip impedance. This phenomenon is usual for an electrically small antenna as the radiation resistance of an antenna is directly proportional to the antenna size.

In the following part, a parametric analysis has been conducted to study the effects of the design parameters. With reference to Fig. 8, the impedance curve is seen to shift toward high frequency in response to an increase in the loop's width (d_2). This is expected because increasing the trace width makes the matching loop become less inductive. Similar effects are observed when the dimensions of the radiating arms (a_3 and b_3) are varied, as illustrated in Fig. 9. Fig. 10 shows the changes in the input impedance with respect to variation in the patches' length (b_5). Increasing b_5 causes the folded dipole to become electrically longer. As such, the resonant frequency is seen to shift down to a lower frequency.

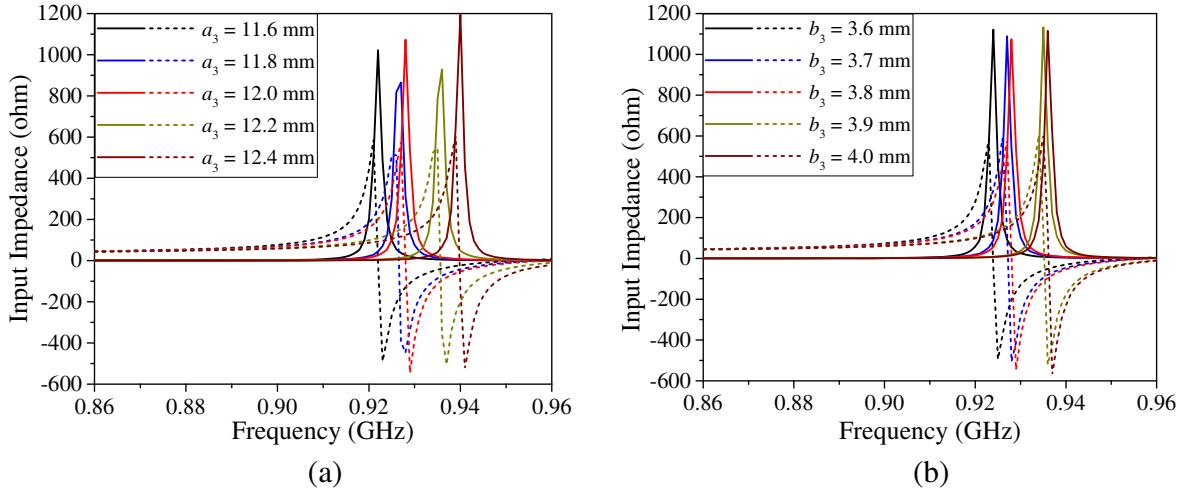


Figure 9. Effects of changing the dimensions of the radiating arms on the input impedance.

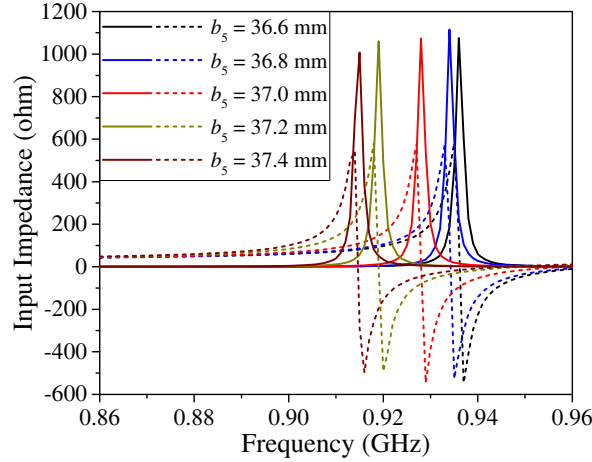


Figure 10. Effects of changing the patches' length (b_5) on the input impedance.

4. MEASUREMENT SETUP

Prototype of the proposed antenna is fabricated, and its tag sensitivity (P_{tag}), read distance (r_{max}), realized gain (G_r), and read pattern are measured using the Voyantic Tagformance system, as showed in Fig. 11. Prior to the tag-under-test measurement, the system is calibrated using a UHF reference tag in the frequency range of 0.86–0.96 GHz. This is to ensure that the background noise level is lower than -60 dBm [22], a condition where the interior of the anechoic chamber can be treated as an open environment that is free from multipath fading and external interferences. Referring to Fig. 11(b), a linearly polarized reader antenna is located in the boresight direction of the tag antenna, and the rating power is 4 W Effective Isotropic Radiated Power (EIRP). The proposed tag antenna is mounted at the center of a metal plate with a size of $20\text{ cm} \times 20\text{ cm}$ on a rotator. While fixing the reader antenna at a constant distance along the z -axis, the tag antenna is allowed to rotate about its own x -, y -, and z -axes to obtain yz -, xz -, and xy -planes, respectively. It should be mentioned that the definitions of the xz - and yz -planes are similar to those for the conventional spherical coordinate system. However, the read pattern in the xy -plane reveals the polarization characteristics of the tag antenna in the boresight direction. During the measurement, the reader antenna changes its transmitted power gradually until a backscattered power is received from the tag. This power is the threshold of the reader's transmitted

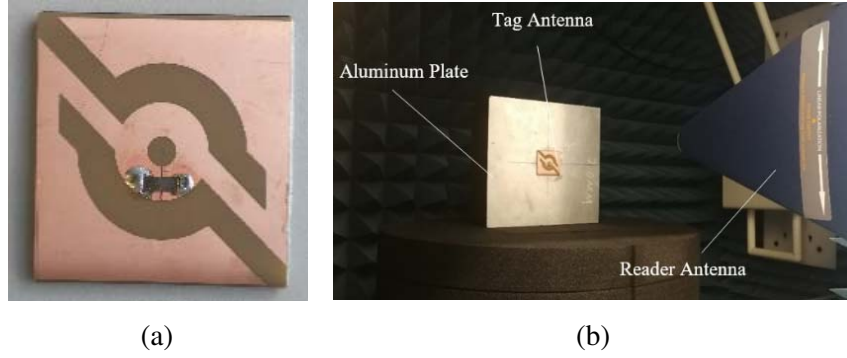


Figure 11. (a) Prototype of the proposed tag antenna. (b) Measurement setup in an anechoic cabinet.

power (P_{th}) which is sufficient to turn on the tag. Then, the realized gain and read distance of the proposed tag antenna are determined using Eqs. (4) and (5), respectively.

$$G_r = \frac{P_{IC}}{L_{fwd}P_{th}}, \quad (4)$$

$$r_{\max} = \frac{\lambda}{4\pi} \sqrt{\frac{P_t G_t G_r}{P_{IC}}}. \quad (5)$$

where P_{IC} is the chip sensitivity, L_{fwd} the forward-link loss where cable and free space losses are included, P_t the power transmitted by the reader, and G_t the gain of the transmitting antenna [23].

5. RESULTS AND DISCUSSIONS

Figure 12 shows the measured read distance and the corresponding tag sensitivity of the proposed tag antenna. Referring to Fig. 12, the maximum achievable read distance is found to be 6.9 m at the resonant frequency of 907 MHz. The measured realized gain and tag sensitivity at resonance are found to be -9.4 dBi and -10.6 dBm, respectively. Slight deviation is observed between the measured and simulated resonant frequencies, which could be caused by imperfections in the fabrication processes. Despite having a small footprint, the achievable read distance of the proposed folded dipole is much longer than most of the conventional metal tags. It is shown that the two-fold rotational symmetry design is useful for miniaturizing the antenna size and enhancing the radiation performances.

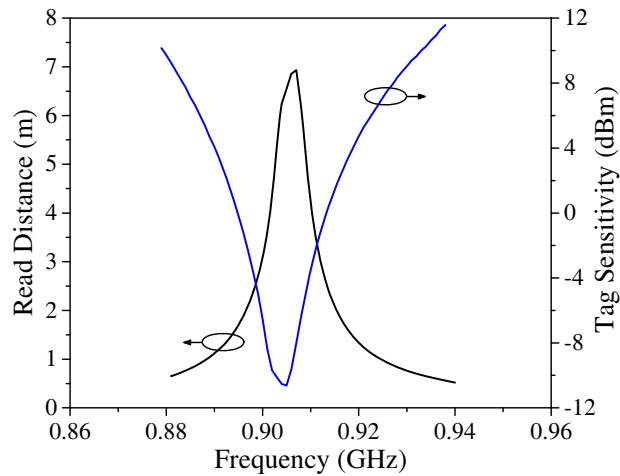


Figure 12. Measured read distance and tag sensitivity of the proposed tag antenna.

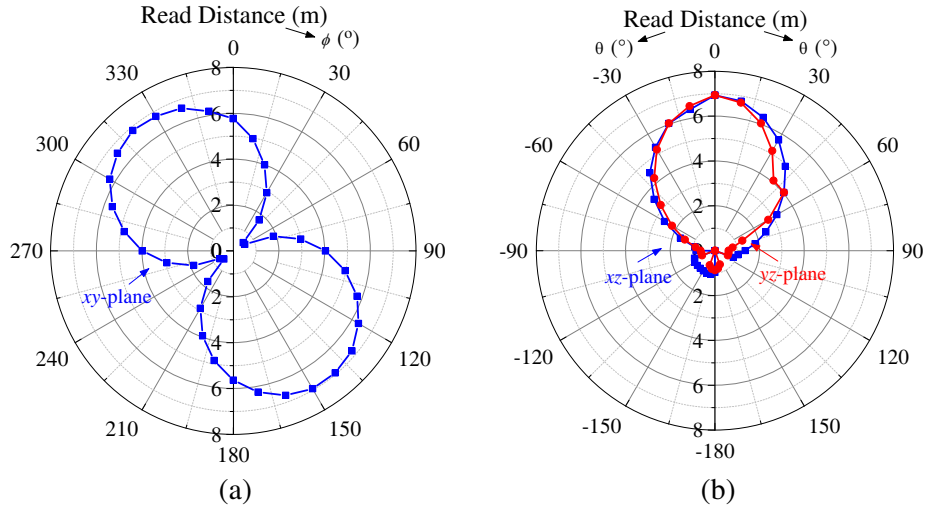


Figure 13. Measured read patterns when the tag antenna is tested on a 20 cm × 20 cm metal plate at 907 MHz. (a) *xy*-plane, (b) *xz*-plane and *yz*-plane.

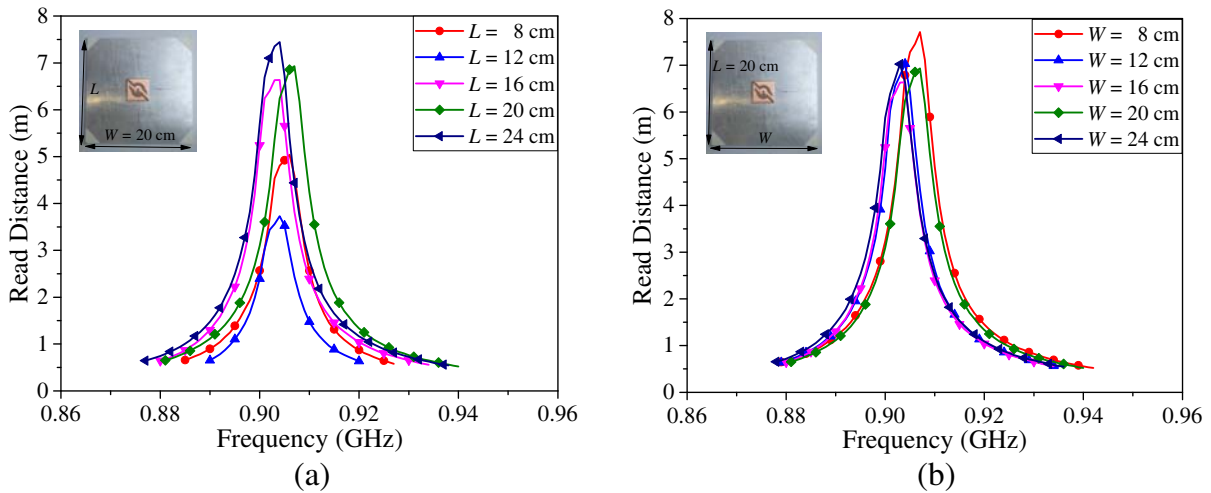


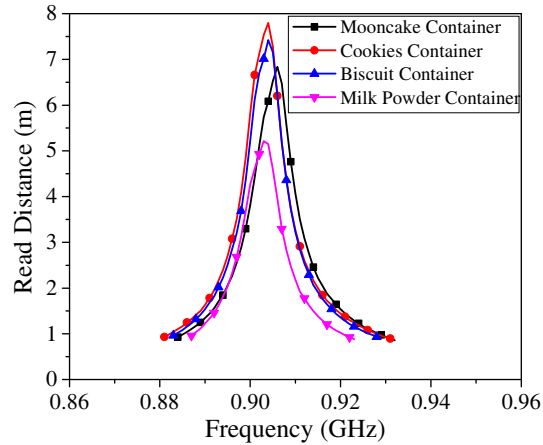
Figure 14. Measured read distances of the proposed tag antenna for different (a) *L* and (b) *W*.

Figure 13 shows the polarization characteristics and radiation patterns of the proposed tag antenna in terms of read distances. As shown in Fig. 13(a), the read distance is found to peak with a value of 6.9 m at $\phi = 140^\circ$ and $\phi = 320^\circ$. This indicates that the proposed tag antenna is linearly polarized, and its polarization angle is 140° from the $+x$ -axis. Referring to the read patterns shown in Fig. 13(b), it can be seen that the radiation is mainly distributed in the upper half-plane with a maximum value detected in the boresight direction. Almost no signals are detected in the lower half-plane, which can be attributed to the existence of the metal plate.

The read distances of the tag with different plate sizes are measured from the boresight direction ($\theta = 0^\circ$), and the results obtained are shown in Fig. 14. As can be seen from Fig. 14, the achievable read distances are mostly in the range of 7 m for various plates with different lengths (*L*) and widths (*W*). This is not something unusual. Since the ground plane of the tag antenna is electrically connected to the copper plate, increasing the plate size will cause the ground plane to increase, and it makes the antenna characteristics converge to that for the infinitely large ground plane [24]. Referring to the same figure, the resonant frequencies of the tag are found distributed in a small range from 903 MHz to 911 MHz. It is shown that the incorporated ground plane underneath is effective for isolating electromagnetic waves,



(a)



(b)

Figure 15. (a) Household metallic containers. (b) Measured read distances of proposed tag antenna on different household metallic containers.

making the proposed structure a platform-tolerant tag antenna.

The proposed tag antenna is also tested on several common household items with different dimensions and shapes in order to check its practicability in RFID tracking and identification, as shown in Fig. 15(a). Again, the read distances are measured in the boresight. As can be seen from Fig. 15(b), all of the tested household items have read distances more than 7 m, except the milk powder container. This is because the milk powder container has relatively smaller tagging than others. The resonant frequency of the tag antenna is rather stable at 907 MHz, which is consistent with the observation in Fig. 14.

The proposed tag antenna is also compared in Table 1 with a couple of contemporary metal-mountable UHF tags available in the literature. The folded dipoles presented in [5, 25] are indeed much smaller than an ordinary half-wavelength dipole. However, not many objects can be tagged by these tags as they have a large footprint, which is about three times larger than ours. In addition, the achievable read distances are not more than 5 m when the tags are placed on metal. Deterioration in the read distance can be due to current cancellation in the closely packed striplines of the folded dipoles. Unlike the previous two, the tag antennas in [18, 26, 27] are designed using quarter-wave antennas for achieving miniaturization. However, these tag antennas are still electrically large, and they have very limited tagging applications. In terms of achievable read distance, the tag antenna presented in [27] is much better than the current work. However, this tag antenna has multiple conductive layers that are sandwiching different substrates, which can be difficult to handle in mass production. Furthermore, the usage of shorting vias in the design may easily boost production costs, which is not for low-cost RFID tagging applications.

Table 1. Comparison of different UHF metal-mountable tags.

	Power	Tag Size (mm)	Substrate	Backing Plate Size (cm)	Max. Read Distance (m)
This work	4 W (EIRP)	40 × 40 × 3.1	PET foam ($\epsilon_r = 1.06$)	20 × 20	6.9
[5]	3.28 W (EIRP)	125.5 × 14 × 1.5	FR4 ($\epsilon_r = 4.3$)	40 × 40	5.0
[18]	1 W (EIRP)	80 × 25 × 3.5	FR4 ($\epsilon_r = 4.7$)	20 × 20	5.0
[25]	4 W (EIRP)	106 × 40 × 1.6	FR4 ($\epsilon_r = 4.7$) + Foam	40 × 40	2.9
[26]	4 W (EIRP)	96 × 50 × 2	FR4 ($\epsilon_r = 4.7$)	20 × 20	4.3
[27]	4 W (EIRP)	72.1 × 25.5 × 3.2	Foam ($\epsilon_r = 1.1$)	20 × 20	8.9

6. CONCLUSION

In this paper, a miniature folded dipole has been proposed for designing a metal-mountable RFID tag. Folding the dipole arms into a rotational symmetry constellation, rather than meandering them, is found able to miniaturize the antenna dimension to not more than one-eighth of wavelength. Capacitive coupling between the arms has been shown to be effective for enhancing the read performance in the boresight. Despite being electrically small, the tag is able to achieve a long read distance of ~ 7 m on metal, which can be attributed to the application of two-fold rotational symmetry in the antenna design. Insignificant shift in the resonant frequency when it is tested with different household items shows that the proposed tag antenna is platform-tolerant.

REFERENCES

1. Chawla, V. and D. Ha, "An overview of passive RFID," *IEEE Commun. Mag.*, Vol. 45, No. 9, 11–17, Sep. 2007.
2. Athauda, T. and N. Karmakar, "Chipped versus chipless RF Identification: A comprehensive review," *IEEE Microw. Mag.*, Vol. 20, No. 9, 47–57, Sep. 2019.
3. Bjorninen, T., L. Sydanheimo, L. Ukkonen, and Y. Rahmat-Samii, "Advances in antenna designs for UHF RFID tags mountable on conductive items," *IEEE Antennas Propag. Mag.*, Vol. 56, No. 1, 79–103, Feb. 2014.
4. Lee, Y. H., E. H. Lim, F. L. Bong, and B. K. Chung, "Bowtie-shaped folded patch antenna with split ring resonators for UHF RFID tag design," *IEEE Trans. Antennas Propag.*, Vol. 67, No. 6, 4212–4217, Jun. 2019.
5. Genovesi, S. and A. Monorchio, "Low-profile three-arm folded dipole antenna for UHF band RFID tags mountable on metallic objects," *IEEE Antennas Wirel. Propag. Lett.*, Vol. 9, 1225–1228, Dec. 2010.
6. Cho, C., H. Choo, and I. Park, "Design of planar RFID tag antenna for metallic objects," *Electron. Lett.*, Vol. 44, No. 3, 175–177, Jan. 2008.
7. Gao, B. and M. M. F. Yuen, "Passive UHF RFID packaging with electromagnetic band gap (EBG) material for metallic objects tracking," *IEEE Trans. Compon. Packaging Manuf. Technol.*, Vol. 1, No. 8, 1140–1146, Aug. 2011.

8. Park, I. Y. and D. Kim, "Artificial magnetic conductor loaded long-range passive RFID tag antenna mountable on metallic objects," *Electron. Lett.*, Vol. 50, No. 5, 335–336, Feb. 2014.
9. Marrocco, G., "Gain-optimized self-resonant meander line antennas for RFID applications," *IEEE Antennas Wireless Propag. Lett.*, Vol. 2, 302–305, 2003.
10. Reed, S., L. Desclos, C. Terret, and S. Toutain, "Patch antenna size reduction by means of inductive slots," *Microw. Opt. Technol. Lett.*, Vol. 29, No. 2, 79–81, Apr. 2001.
11. Chen, H. M., S. A. Yeh, Y. F. Lin, S. C. Pan, and S. W. Chang, "High chip reactance matching for ultra-high-frequency radio frequency identification tag antenna design," *IET Microw., Antennas Propag.*, Vol. 6, No. 5, 577–582, Apr. 2012.
12. Shen, P., W. R. Zhang, L. Huang, D. Y. Jin, and H. Y. Xie, "Improving the quality factor of an RF spiral inductor with non-uniform metal width and non-uniform coil spacing," *J. Semicond.*, Vol. 32, No. 6, 1–5, Jun. 2011.
13. Koo, T. W., D. Kim, J. I. Ryu, H. M. Seo, J. G. Yook, and J. C. Kim, "Design of a label-typed UHF RFID tag antenna for metallic objects," *IEEE Antennas Wireless Propag. Lett.*, Vol. 10, 1010–1014, Aug. 2011.
14. Bong, F. L., E. H. Lim, and F. L. Lo, "Miniaturized dipolar patch antenna with narrow meandered slotline for UHF tag," *IEEE Trans. Antennas Propag.*, Vol. 65, No. 9, 4435–4442, Sep. 2017.
15. Babar, A. A., T. Björninen, V. A. Bhagavati, L. Sydänheimo, P. Kallio, and L. Ukkonen, "Small and flexible metal mountable passive UHF RFID tag on high-dielectric polymer-ceramic composite substrate," *IEEE Antennas Wireless Propag. Lett.*, Vol. 11, 1319–1322, Nov. 2012.
16. Lee, Y. H., E. H. Lim, F. L. Bong, and B. K. Chung, "Folded antipodal dipole for metal-mountable UHF tag design," *IEEE Trans. Antennas Propag.*, Vol. 66, No. 11, 5698–5705, Nov. 2018.
17. Choi, Y., U. Kim, J. Kim, and J. Choi, "Design of modified folded dipole antenna for UHF RFID tag," *Electron. Lett.*, Vol. 45, No. 8, 387–389, Apr. 2009.
18. Yang, P. H., Y. Li, L. Jiang, W. C. Chew, and T. T. Ye, "Compact metallic RFID tag antennas with a loop-fed method," *IEEE Trans. Antennas Propag.*, Vol. 59, No. 12, 4454–4462, Dec. 2011.
19. "Monza R6 tag chip datasheet," document IPJ-W1700, Impinj, Inc., Seattle, WA, USA, 2016.
20. Niew, Y. H., K. Y. Lee, E. H. Lim, F. L. Bong, and B. K. Chung, "Patch-loaded semicircular dipolar antenna for metal-mountable UHF RFID tag design," *IEEE Trans. Antennas Propag.*, Vol. 67, No. 7, 4330–4338, Jul. 2019.
21. "ECCOSTOCK PP," Accessed on Jan. 2018, [Online]. Available: <http://www.eccosorb.com/Collateral/Documents/English-US/PP.pdf>.
22. Rao, K. V. S. and P. V. Nikitin, "Theory and measurement of backscattering from RFID tags," *IEEE Antennas Propag. Mag.*, Vol. 48, No. 6, 212–218, Dec. 2006.
23. Rao, K. V. S., P. V. Nikitin, and S. F. Lam, "Antenna design for UHF RFID tags: A review and a practical application," *IEEE Trans. Antennas Propag.*, Vol. 53, No. 12, 3870–3876, Dec. 2005.
24. Lee, Y. H., E. H. Lim, F. L. Bong, and B. K. Chung, "Compact folded C-shaped antenna for metal-mountable UHF RFID applications," *IEEE Trans. Antennas Propag.*, Vol. 67, No. 2, 765–773, Feb. 2019.
25. Xu, L., B. J. Hu, and J. Wang, "UHF RFID tag antenna with broadband characteristic," *Electron. Lett.*, Vol. 44, No. 2, 79–80, Jan. 2008.
26. Mo, L., H. Zhang, and H. Zhou, "Broadband UHF RFID tag antenna with a pair of U slots mountable on metallic objects," *Electron. Lett.*, Vol. 44, No. 20, 1173–1174, Sep. 2008.
27. Son, H. W. and S.-H. Jeong, "Wideband RFID tag antenna for metallic surfaces using proximity-coupled feed," *IEEE Antennas Wireless Propag. Lett.*, Vol. 10, 377–380, Apr. 2011.